Physical Parameters in High-Accuracy Spectrophotometry

K. D. Mielenz

Optical Physics Division, Institute for Basic Standards, National Bureau of Standards, Washington, D.C. 20234

The measured apparent transmittance T_A of a filter or liquid sample depends on the beam geometry in the spectrophotometer. For focused light incident upon the sample, T_A is different for systems having different f-numbers, and also depends on the state of polarization of the light. These effects are eliminated when the incident light is collimated; in this case T_A approaches the "true" transmittance τ of the sample. Both modes of operation suffer from stray light and interference effects. The former may be reduced significantly by using mirror rather than lens optics, and the latter by suitable choice of the monochromator slit width. A new spectrophotometer based upon the above-mentioned design principles is described. The photometric precision of this instrument is shot-noise limited, permitting measurements to better than 10^{-4} transmittance units.

The double-aperture method of testing detector linearity to this level of precision is discussed. The conventional method of finding the nonlinearity correction can be replaced by a curve-fitting procedure giving better precision. Data on detector nonlinearity, and its dependence on wavelength, are presented.

Key words: High accuracy spectrophotometry, physical parameters; linearity test of photodetector; spectrophotometry, high accuracy.

I. Introduction

When the same sample is measured with two spectrophotometers the results often disagree by amounts several times greater than the precision of either instrument. An example of this is given in table 1, summarizing a recent NBS in-house intercomparison of two spectrophotometers both of which have precisions well below 10^{-4} transmittance units. When the measurements were repeated, it was found that the

TABLE 1. Results of comparative filter measurements. The high-accuracy spectrophotometers described in reference [1] and in this paper were used for this test

	Measured transmittance				Range of nonuniformity of filter (635 nm)
	440 nm	465 nm	590 nm	635 nm	
10% Filter					
Lab 1	0.1159	0.1356	0.1037	0.1136	
Lab 2	0.1145	0.1339	0.1024	0.1122	0.0005
Diff.	+ 0.0014	+ 0.0017	+ 0.0013	+ 0.0014	
20% Filter					
Lab 1	0.1980	0.2259	0.1916	0.2060	
Lab 2	0.1980	0.2259	0.1916	0.2061	0.0004
Diff.	0.0000	0.0000	0.0000	0.0001	
30% Filter					
Lab 1	0.3287	0.3553	0.3113	0.3255	
Lab 2	0.3289	0.3557	0.3115	0.3258	0.0001
Diff.	− 0.0002	− 0.0004	− 0.0002	− 0.0003	

filters were slightly inhomogeneous. This inhomogeneity is too small to account for the relatively large discrepancies for the 10 percent filter, but large enough to dismiss the agreement on the 20 percent filter as fortuitous, since no attempt had been made to measure the same area of these filters. Furthermore, the filters were found to be slightly dichroic in one laboratory, but not in the other. A similar interlaboratory test, which led to a small residual bias of roughly the same magnitude, is reported in reference [1].[1]

For the purposes of routine spectrophotometry, the level of agreement of these measurements is quite satisfactory, but not from the point of view of high-accuracy spectrophotometry. With well-designed modern spectrophotometers, it is possible to achieve repeatabilities of a few 10^{-5} transmittance units. Anyone using such advanced instrumentation cannot ignore discrepancies as large as those mentioned. As other cooperative tests have shown before [2], the above-mentioned results indicate that a part of the discrepancies must be attributed to the samples used. In view of this difficulty, spectrophotometric accuracy cannot be assessed by interlaboratory tests alone. In order to separate the effects of sample and instrument, it is necessary to identify the various possible sources of systematic errors for each of the spectrophotometers involved, and to take them into account before comparing results.

The main emphasis of this paper is on systematic errors due to beam geometry. It will be shown that different spectrophotometers are, indeed, likely to give different results. Conversely, it is entirely possible to obtain agreement between two instruments of similar design, but what was measured may not have been a meaningful material property of the sample.

Some of the beam-geometry errors are calculable by straightforward application of optical physics. These may be eliminated by numerical correction of the measured results. In other cases, the magnitude of the error must be determined experimentally. Ideally, a high-accuracy spectrophotometer should have off-axis mirror optics, and all measurements should be made in parallel light. Nevertheless, it is possible, although significantly more difficult, to perform accurate measurements using a conventional focused-beam spectrophotometer with lenses. Both types of instruments may suffer from systematic errors due to interference.

The particular samples discussed are glass filters, because these appear to be the most commonly used transfer standards for assessing spectrophotometric accuracy. A definition is given of what might be considered the 'true' transmittance of an ideal filter, followed by a discussion of some of the pitfalls of real filters.

The necessity to eliminate the systematic error due to nonlinear detector response is well recognized. It will be shown that the double-aperture [3] method can be adapted to yield the additive nonlinearity correction to $\pm 1 \times 10^{-5}$ transmittance units.

II. A New Spectrophotometer

Most of the measurements reported in this paper were performed with a new single-beam spectrophotometer designed as a research tool for spectrophotometric measurements with an accuracy exceeding that of conventional systems. The instrument is described elsewhere [4, 5] in greater detail; its design is shown schematically in figure 1.
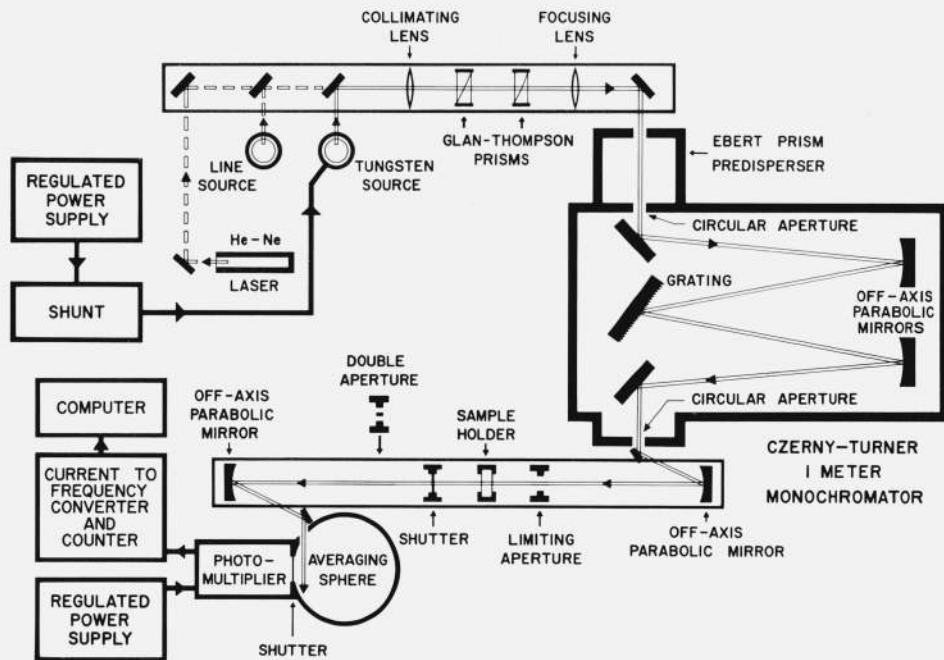

FIGURE 1. High-accuracy spectrophotometer.

---

[1] Figures in brackets indicate the literature references at the end of this paper.

The monochromator is an f/8.7 Czerny-Turner system with 1-m off-axis parabolic mirrors and a 1200-lines/mm plane grating blazed for 500 nm. The entrance and exit 'slits' are interchangeable circular apertures with diameters ranging between 0.25 and 1 mm, so that the exit aperture approximates a point source having a spectral band pass between 0.2 and 0.8 nm when the grating is used in the first order. This light is collimated by a 195-mm off-axis parabolic mirror, and focused into the detector by another. These two mirrors are mounted at the ends of a 120-cm precision optical bench; the space between them constitutes the sample compartment of the spectrophotometer. It will become apparent in this paper that this design; namely, the exclusive use of off-axis mirror optics, and the placement of the sample in a collimated and linearly polarized beam, constitutes the optimal beam geometry for high-accuracy spectrophotometry.

A large sample space was provided in this spectrophotometer, so that the beam geometries of other instruments can be simulated by means of lenses placed in the collimated beam. Several of the measurements reported in this paper were performed in this manner.

The light source is a tungsten ribbon lamp, rated for 6V and 18A, and connected to a regulated power supply using external sensing on a 0.1 Ω shunt rated for 50 A. Except for a possible linear drift in time, the radiant-flux output of this source is constant to better than 0.01 percent for periods of the order of 20 min. The flux into the monochromator is varied by variation of the lamp current or rotation of the first of the two Glan-Thompson prisms shown in figure 1. The second Glan-Thompson prism defines the state of polarization of the light. The source is focused on the entrance slit of the Ebert prism predisperser which precedes the grating monochromator.

A 2-mW helium-neon laser was installed in the system for alignment purposes, and spectral lamps are provided for calibration of the wavelength scale to a 0.02-nm accuracy.

The detector is an end-on photomultiplier tube attached to a 15-cm averaging sphere with an estimated efficiency of 20 percent. The photomultiplier tube has an S−20 cathode and 11 stages; the dynode chain is linear with a Zener diode between cathode and first dynode. Its power supply is voltage-regulated to 0.001 percent, and the anode current is measured by a current-to-frequency converter similar to that described by Taylor [6]. This converter and its associated high-precision counter were found to be linear to better than one part in 10^4, and to have a full-scale repeatability less than two parts in 10^5. The counter integrates over a 10-s interval.

The counter signals are recorded automatically on punched paper tape by means of a data acquisition and control system, which is also used as a computer terminal to process the recorded data.

Upon construction of the spectrophotometer, a series of tests was undertaken to determine its photometric precision. The signal currents generally drifted in time and exhibited random fluctuations superimposed upon this drift. Since all quantities measured with a spectrophotometer are ratios, the drift is of no concern provided it is linear in time, and provided that all readings are taken at fixed time intervals. Under these conditions the quantity affecting the precision of transmittance measurements is the standard deviation,

$$dI = \left\{ \sum_{\nu=1}^{n} [I_\nu - I(\nu t)]^2 / (n-1) \right\}^{1/2} \quad (1)$$

where $I_1, I_2, \ldots I_n$ are n successive readings of the same signal current I, and $I(\nu t)$ is their expectation value, obtained from a least-square fit of the measured data as a linear function of time, t.
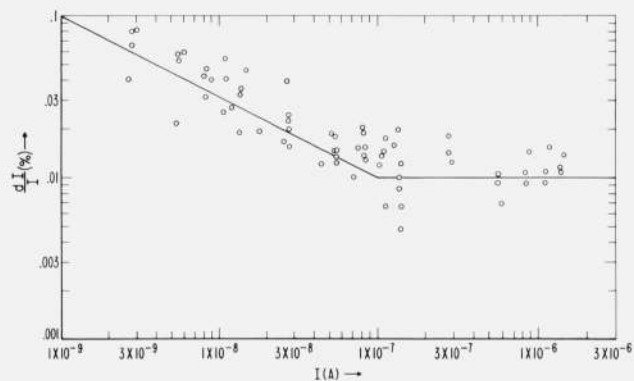

FIGURE 2. Photometric precision dI/I of spectrophotometer versus signal current I.

When plotted as shown in figure 2, the random error, dI, so defined, was found to be primarily a function of the signal current, I, itself independent of the particular combinations of lamp current, flux attenuation, wavelength, and photomultiplier dynode voltage used to produce any particular value of I. As indicated by the solid line, the relationship between dI and I is, approximately,

$$dI/I = \begin{cases} \sqrt{10/I} \times 10^{-7} & \text{if } I < 10^{-7} \text{ A}, \quad (2a) \\ 10^{-4} & \text{if } I > 10^{-7} \text{ A}, \quad (2b) \end{cases}$$

The low-current branch (2a) of this curve is due to photomultiplier shot noise. The limiting value (2b) for large signal currents is attributed to lamp noise.

Equations (2a, b) can be used to predict the random error,

$$dT = \left[\left(\frac{dI}{I} \right)^2 + \left(\frac{d(TI)}{TI} \right)^2 \right]^{1/2}, \quad (3)$$

with which this spectrophotometer will perform transmittance measurements. The result is that the standard deviation of a single measurement of transmittance is of the order of 10^{-4} transmittance units or less, provided that the signal current, I, for the 100

457

percent point of the transmittance scale is chosen to be equal or greater than 10^{-7} A. Measurements based on a series of repeated readings will then be reproducible to within a few 0.00001 transmittance units. This expectation was verified directly, when separate transmission measurements of neutral-density glass filters with nominal transmittances of 0.1, 0.2, and 0.3 were found to be repeatable to ± 0.00004.

III. The 'True' Transmittance of a Filter

The optical transmittance of a given sample,

$$T = \frac{\text{transmitted radiant flux}}{\text{incident radiant flux}}, \qquad (4)$$

is not a well-defined property of matter. It depends on the form of the sample, on the path which the light travels, and is also a function of the polarization and degree of coherence of the light. Thus, it cannot serve a useful purpose in spectrophotometry unless constraints are imposed on sample and light beam so that the above ratio of fluxes is reduced to a meaningful material property. In the following, this limiting form of the optical transmittance, T, will be referred to as the 'true' transmittance, τ, of the sample.

As an example, consider an ideal glass filter; that is, a plane-parallel slab of homogeneous material of complex refractive index $\hat{n} = n(1 + i\kappa)$ and thickness,
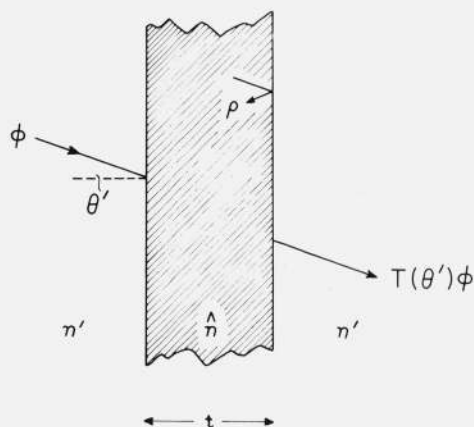

FIGURE 3. Notation used in calculating the transmittance of a filter.

t, bordered by identical media with refractive index, n', and illuminated by a linearly polarized plane wave of wavelength λ and angle of incidence θ' (fig. 3). Its optical transmittance is [7]

$$T(\theta') = \left| \frac{(1 - \rho^2) e^{i\beta}}{1 - \rho^2 e^{2i\beta}} \right|^2 \qquad (5a)$$

where ρ is the appropriate Fresnel coefficient of amplitude reflection at each of the two boundary surfaces, given by

$$\rho_\perp = \frac{n' \cos \theta' - \hat{n} \cos \hat{\theta}}{n' \cos \theta' + \hat{n} \cos \hat{\theta}} \qquad (5b)$$

for S-polarization and

$$\rho_\parallel = -\frac{n' \cos \hat{\theta} - \hat{n} \cos \theta'}{n' \cos \hat{\theta} + \hat{n} \cos \theta'} \qquad (5c)$$

for P-polarization. Furthermore,

$$\beta = (2\pi/\lambda) t \hat{n} \cos \hat{\theta}, \qquad (5d)$$

with $\hat{\theta}$ defined by Snell's law,

$$\hat{n} \sin \hat{\theta} = n' \sin \theta'. \qquad (5e)$$

These equations indicate that T is a function of the angle of incidence and state of polarization of the light. Therefore, different transmittances may be measured for the same sample with spectrophotometers for which the angles of light incidence are different. In addition, the measured transmittance may vary when the polarization of the light is varied, so that a nonpolarizing filter may exhibit an instrument-dependent, apparent dichroism.

Equation (5a), which is based on the assumption of perfectly coherent light, also leads to an interference term. In practice, the degree of coherence of the light is different for different spectrophotometers, so that the actually observed interference effect will be more or less subdued. This may lead to further instrumental discrepancies of measured transmittances.

These sources of error are eliminated when transmittance is measured in collimated light at normal incidence, and under conditions such that interference is negligible. Then, eq (5a) is reduced to

$$T(0) = \frac{(1 - r)^2 \tau_i}{1 - r^2 \tau_i^2} \equiv \tau, \qquad (6a)$$

where r is the energy reflectance at normal incidence, given by

$$r = |\rho_\perp|^2 = |\rho_\parallel|^2 = \left| \frac{n' - \hat{n}}{n' + \hat{n}} \right|^2 \qquad (6b)$$

for either state of polarization, and where

$$\tau_i = e^{-4\pi n \kappa t/\lambda} \qquad (6c)$$

is the internal transmittance of the filter for normal incidence.

Equation (6a) is a function of the filter parameters, $\hat{n}$ and t, only [8], and may therefore be identified as the above-mentioned 'true' transmittance, τ, of the filter. Any departures of measured transmittance from this value of τ are to be considered errors.

458

IV. Requirements for Standard Filters

A few simple conclusions from eqs (6a, b, c) may serve here to demonstrate some of the difficulties in assessing spectrophotometric accuracy by measuring the same sample in different laboratories.

Differentiation of eq (6c) shows that the variation of τ_i due to a variation of sample thickness, t, is

$$\Delta\tau_i = \tau_i(\ln \tau_i)\Delta t/t, \tag{7}$$

which has an extreme value, $\Delta\tau_i = -0.37\Delta t/t$, if $\tau_i = 0.37$. Hence, it may be seen that t must be constant to at least 0.5 μm if the transmittance of a 2-mm thick filter is to be constant to 10^{-4} transmittance units. The filter must be plane-parallel to 0.1 milliradians if this requirement is to be satisfied over a 5-mm area. Equally stringent requirements must, of course, be imposed on the homogeneity of the filter material.

The importance of proper sample handling and cleaning may be illustrated by assuming the presence of a thin contaminating layer of thickness, t_1, and refractive index, n_1, on the filter surfaces. In this case, the Fresnel reflectance, r, in eq (6a) must be replaced by [9]

$$r_1 = \frac{n_1^2(n'-n)^2 + (n_1^2 - n'^2)(n_1^2 - n^2)\sin^2(x/2)}{n_1^2(n'+n)^2 + (n_1^2 - n'^2)(n_1^2 - n^2)\sin^2(x/2)}$$

$$\sim \frac{(n'-n)^2}{(n'+n)^2}\left\{1 + \frac{4n'n(n_1^2 - n'^2)(n_1^2 - n^2)}{n_1^2(n'-n)^2(n'+n)^2}\sin^2(x/2)\right\}$$

$$\tag{8a}$$

where

$$x = 4\pi n_1 t_1/\lambda, \tag{8b}$$

and where it was assumed that $\kappa \ll 1$ and that $(n_1^2 - n'^2)(n_1^2 - n^2)/n_1^2(n'+n)^2$ is a small number [10]. In practice, the film may be water ($n_1 \sim 1.33$), oil ($n_1 \sim 1.47$), or some similar contaminant, so that $n_1 \sim 1.4$ may be taken as an average representative number. If $n' \sim 1$ and $n \sim 1.5$, then $r_1 \sim r - 12 \sin^2(x/2)$, with r as the Fresnel reflectance (6b) of the uncontaminated surfaces. Hence, it is seen that the film acts as an anti-reflection coating; its effect on transmittance will be less than 10^{-4} transmittance units only if $2(r-r_1) \leqslant 10^{-4}$. According to (8b), the corresponding tolerance on the film thickness is $t_1 \leqslant 2 \ 10^{-3} \lambda$, so that a layer only a few molecules thick may be troublesome. Repeated cleaning is likely to leave residual layers of at least this magnitude on the filter surfaces. A similar difficulty arises from the fact that the surfaces may gradually become leached by certain cleansing agents. The additional problem of dust is too well known to deserve more than passing mention at this point.

These examples show the large effect that inadequate samples and sample handling techniques may have on interlaboratory comparisons. Efforts are being made to develop more homogeneous filter materials, and to grind and polish them with greater precision, [11]. In the meantime some improvement may be achieved by more elaborate calibration procedures; for example, the calibration of a standard filter should be done by mapping. The filters must be cleaned with properly selected chemicals. They should also be recalibrated periodically, so that the user is made aware of any surface damage or accumulation of residual layers.
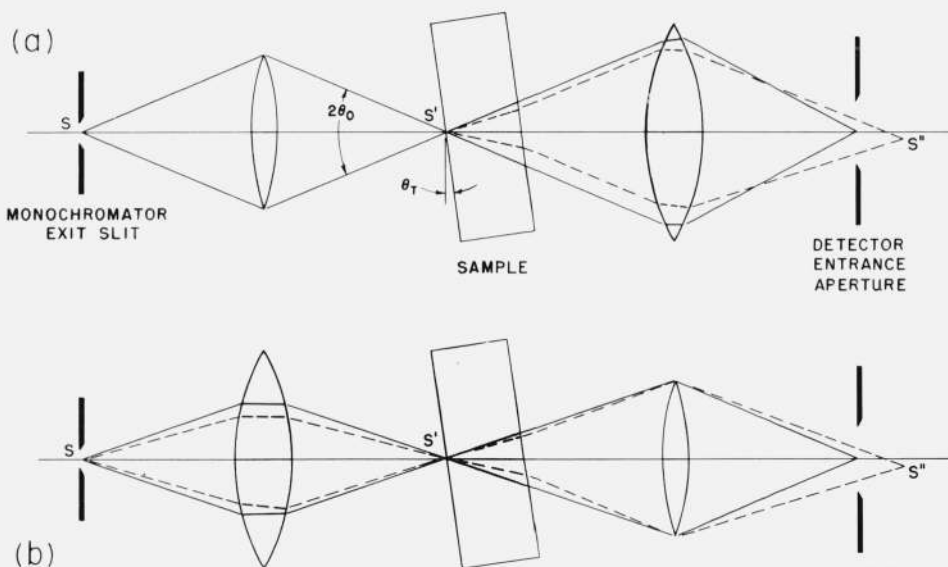

FIGURE 4. Path of light in focused-beam spectrophotometer before (———) and after (- - - - -) sample was inserted, and with (a) the first lens, and (b) the second lens as the limiting aperture.

V. Beam-Geometry Effects

The sample compartment of many spectrophotometers is designed as shown in figure 4, where the monochromator exit slit is focused into the sample by a lens, and is refocused into the detector by another. This beam geometry is preferred by most designers for intensity reasons (all of the flux from the slit is passed through the sample), but it will not yield the 'true' transmittance τ of eq (6a). The major systematic errors inherent in this design are due to beam displacement, interreflections, and oblique light incidence. These errors will be discussed now, in order to establish the conditions for which they are either negligibly small or may be eliminated by numerical correction.

A. Beam-Displacement Errors

The solid lines in figures 4a, b, show the path of light in a focused-beam spectrophotometer without the sample. As indicated by the broken lines, the sample shortens the effective distance between the intermediate slit image, S', and the second lens by an amount $t(1-1/n)$, so that the final slit image, S'', is shifted towards the detector. If the sample is not normal to the optic axis, S'' will also be shifted laterally. This causes different areas of the detector surface to be illuminated before and after the sample was inserted and, therefore, leads to errors because most detectors show a variation of sensitivity with illuminated area. This error must be avoided by passing the light through an averaging sphere before it reaches the detector. While this is a well-recognized fact, it is surprising that even some of the more elaborate commercial spectrophotometers are not equipped with averaging spheres. The inefficiency of spheres in some portions of the spectrum is no adequate reason not to use them at all.

Another error arises when the second lens is the limiting aperture of the beam, as in figure 4b. In this case, the insertion of the sample changes the effective aperture of the first lens, such that it collects less light than without the sample, resulting in too low a measured transmittance. It is easy to show, by measurements with either lens as the limiting aperture, that this error may be quite large. The results of such meaurements, listed in table 2, demonstrate the necessity to underfill the second lens.

TABLE 2. Measured transmittance of three neutral-density filters in focused light with (a) the first lens, and (b) the second lens as the limiting aperture (f/5)

(a)	(b)	(a)−(b)
0.10399	0.10303	0.00096
.31362	.31211	.00151
.58981	.58588	.00393

B. Interreflection Errors

Before the sample is inserted into the beam of a spectrophotometer with lenses, the radiant flux propagated toward the detector is, according to figure 5a,

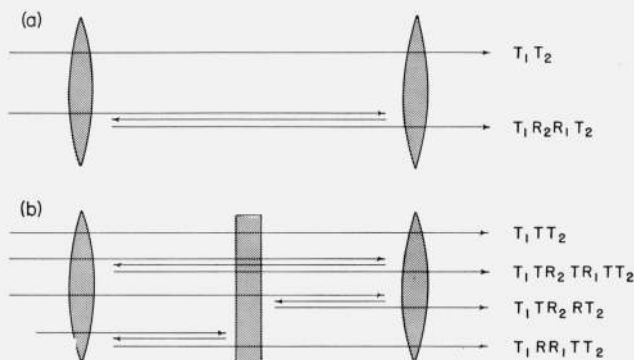$$\phi = T_1 T_2 (1 + R_1 R_2 + \ldots), \qquad (9a)$$

FIGURE 5. Reflected beams in a spectrophotometer with lenses.

where T_1, T_2, R_1, and R_2 are the transmittances and reflectances of the two lenses, and where any contributions due to four or more reflections are considered negligibly small. When the sample is placed in the beam, the transmitted flux is, as indicated in figure 5b,

$$\phi' = T_1 T T_2 (1 + R_1 R_2 T^2 + R R_2 + R_1 R + \ldots), \qquad (9b)$$

with T and R as the transmittance and reflectance of the sample.

As may easily be seen by measuring a sample with and without two clear glass plates on either side of it, the discrepancy between the ratio of these two fluxes and the transmittance, T, of the sample may be quite large. The results of such a measurement are plotted in figure 6, according to which the error is a monotonic function of transmittance and approaches 0.01 transmittance units for large values of T. This experiment represents a particularly bad case, but nevertheless, illustrates the seriousness of interreflection errors.
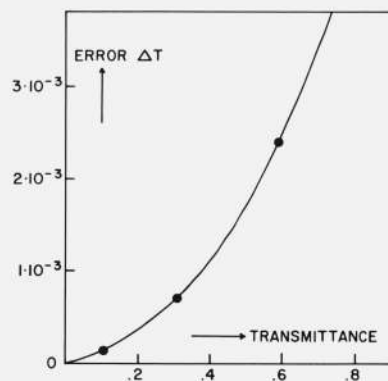

FIGURE 6. Difference ΔT in transmittance for three filters, measured between two clear glass plates and without them.

The main cause of the error is the fact that the insertion of the sample creates the two additional beams shown at the bottom of figure 5b. As is well known, these two beams may be prevented from reaching the detector by tilting the sample. This is indicated in figure 7 for the component reflected from the front surface of the sample and returned by the first lens. If this lens is biconvex, the light is focused into a real image, S_1, by the first surface of the lens, and into a virtual image, S_2, by the second. The
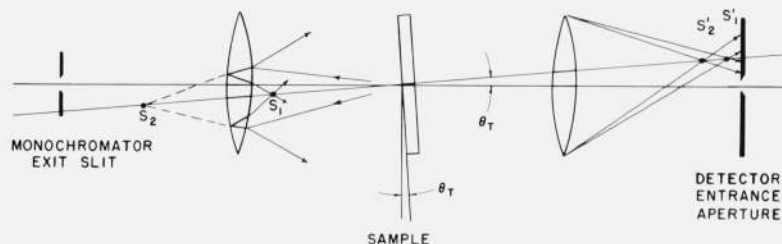
interreflection effect is large. A semireflecting non-absorbing sample may be used. In this case the error, $(\phi'/\phi) - T$, is largest when $R = (1 - T) = 0.5$. According to figure 6, a clear glass or quartz plate also gives a large effect. In both cases, the dependence of reflectance on angle of incidence and polarization must be taken into account; otherwise a plateau may not be found. This is illustrated in figure 8. A 2-mm quartz plate was used, and data were taken for both, S and P polarization in the tilt plane of the

FIGURE 7. Elimination of interreflections by sample tilting.

right-hand side of the figure shows the corresponding images, S_1' and S_2', formed by the second lens, as well as the cones of light that must not pass through the detector entrance aperture. Figure 7 deals with only two of the eight ghost images thus formed, but it is clear that they all lie on the straight line shown, intersecting the optic axis at the tilt angle θ_T. Thus, it is always possible to eliminate the two bottom beams in figure 5b by sufficiently tilting the sample.

Just how much tilt is required is a very complicated function of beam geometry, and is best decided experimentally by measuring transmittance versus tilt angle until a plateau is reached. Such tests should be done under well-defined conditions for which the

sample [12]. According to section 5.3, below, the average of the S and P data is theoretically independent of angle for small values of θ_T. Thus, the figure indicates that a tilt angle of approximately 3° is necessary for this particular instrument.

When enough tilt was introduced, the last two terms in eq (9b) may be omitted. Then the ratio of the two fluxes received by the detector becomes

$$\phi'/\phi = T \frac{1 + R_1 R_2 T^2 + \ldots}{1 + R_1 R_2 + \ldots}$$

$$= T[1 - R_1 R_2 (1 - T^2) + \ldots]. \qquad (10)$$

The residual interreflection error given by this equation, is due to the fact that the direct beam in figure 5b has passed the sample once, whereas the remaining interreflected beam has passed it three times. This error cannot be eliminated by tilting.

Representing amounts of light which actually reach the detector, the quantities R_1 and R_2 in eq (10) are rather complicated functions of beam geometry. Nevertheless, it is clear that the residual error has a maximum, $T - \phi'/\phi = 0.38 R_1 R_2$ for $T = 0.577$, and, therefore, remains below 10^{-4} transmittance units as long as $\sqrt{R_1 R_2} \leq 0.016$. In spite of the difficulty to assign numerical values to R_1 and R_2, it is likely that well-coated lenses will meet this requirement. Whether or not this is the case can be ascertained by means of a standard sample of about 60 percent transmittance which was calibrated on a lensless spectrophotometer.

C. Obliquity Errors

When defocusing and interreflection effects are eliminated, the remaining beam-geometry error of focused-beam spectrophotometers is due to oblique light incidence.
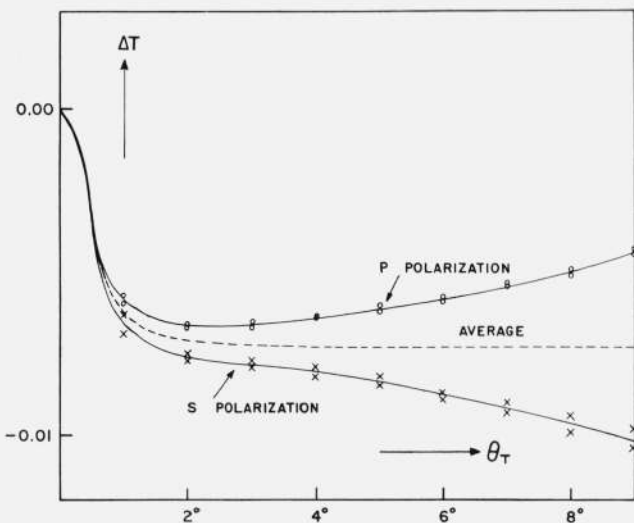

FIGURE 8. Difference ΔT in measured transmittance versus tilt angle for clear glass sample between lenses.

Since θ' and $\hat{\theta}$ are small angles, and since the extinction coefficient, $n\kappa$, is also small, we have

$$\rho_\perp = \frac{n'-n}{n'+n}[1 + (n'/n)\theta'^2].\tag{11a}$$

$$\rho_\parallel = -\frac{n'-n}{n'-n}[1 - (n'/n)\theta'^2].\tag{11b}$$

as obtained by Taylor expansion of eqs (5b, c) to second order in θ' and θ, using Snell's law (5e), and letting $\hat{n} \sim n$. Similarly, eq (5d) leads to

$$\beta = (2\pi/\lambda)nt\{[1 - 1/2(n'\theta'/n)^2] + ik[1 + 1/2(n'\theta'/n)^2]\},\tag{11c}$$

when second-order terms in κ are neglected.

With these approximations, the 'true' transmittance of eq (6a) becomes

$$\tau = \frac{(1-r)^2\tau_i}{1 - r^2\tau_i^2}\tag{12a}$$

with τ_i as given by (6c) and

$$r = \left(\frac{n'-n}{n'+n}\right)^2.\tag{12b}$$

Similarly, eq (5a) is reduced to

$$T[\theta'] = \tau(1 + \gamma_i\theta'^2 \pm \gamma_r\theta'^2),\tag{13a}$$

$$\gamma_i = 1/2(n'/n)^2 \ln \tau_i,\tag{13b}$$

$$\gamma_r = 4(n'/n)r,\tag{13c}$$

where the upper and lower signs in (13a) pertain to S and P polarization, respectively, and where the interference term was again averaged. All terms in r^2 appearing in (13b, c) were neglected.

The two sources of error; namely, a decrease of internal transmittance due to increased path lengths at oblique incidence, and dependence of Fresnel reflectance on angle of incidence, appear as the separate terms involving γ_i and γ_r in (13a). These will be discussed in the following two sections.

1. Path-Length Error—In a focused-beam spectrophotometer, the average path of light through the sample is a function of the sizes and shapes of the monochromator exit slit and of the effective aperture of the focusing lens. In the following, it will be assumed that the slit is sufficiently short to be treated as a point source, and that the lens is underfilled so that the beam cross-section is rectangular because of the rectangular grating or prism aperture. For simplicity, the aperture will be assumed to be square, subtending the same angle $2\theta_0$ in both the horizontal and vertical planes. Furthermore, it will be assumed

that the sample is tilted only in one of these planes. As before, the tilt angle will be denoted by θ_T.

Under these conditions, the average value of the squared angle of incidence θ'^2 in the tilt plane is, according to figure 4a,

$$(\theta'^2)_{av} = \frac{1}{2\theta_\delta}\int_{\theta_T-\theta_0}^{\theta_T+\theta_0} \theta'^2 d\theta' = 1/3(\theta_0^2 + 3\theta_T^2).\tag{14a}$$

In the remaining plane there is no tilt, so that

$$(\theta'^2)_{av} = 1/3\theta_0^2.\tag{14b}$$

The effective value of θ'^2 to be used in eq (13a) is the sum of these two. Therefore, the expected path-length error is

$$\tau - T = -\tau\gamma_i 2/3(\theta_0^2 + 1.5\theta_0^2) = -1/3(n'/n)^2\tau(\ln \tau_i)(\theta_0^2 + 1.5\theta_T^2).\tag{15}$$

If the Fresnel reflectance is small, this function has a maximum at $\tau_i = 0.37$. For this particular value of internal transmittance, and assuming $n = 1.5$, $n' = 1$, its magnitude is $\tau - T = 0.05\ (\theta_0^2 + 1.5\theta_T^2)$,
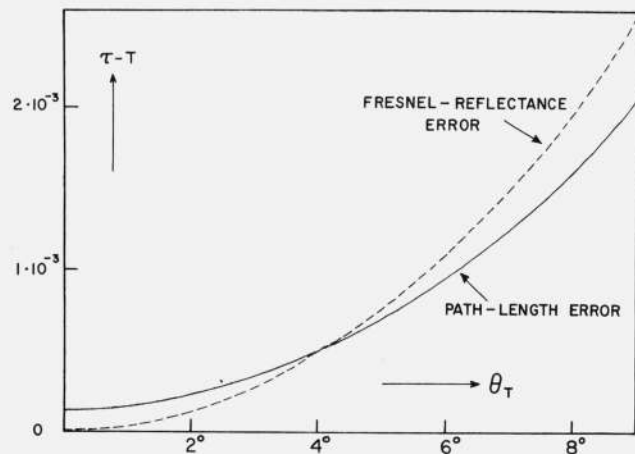

FIGURE 9. Maximal path-length error (for $\tau_i = 0.37$ and $\theta_0 = 0.05$ rad) and maximal Fresnel-reflectance error (for $\tau_i = 1.00$ and P polarization) versus tilt angle θ_T, as computed from eqs (15) and (16) with $n = 1.5$, $n' = 1$.

which is plotted in figure 9 as a function of tilt angle θ_T for an f/10 cone of light ($\theta_0 = 0.05$ rad). The graph shows that the effect of the cone angle, θ_0, is small, but that errors of the order of 10^{-3} transmittance units may be caused when the tilt angle is appreciable.

2. Fresnel-Reflectance Error—According to eq (13a) the effects of S and P polarization are approximately equal in magnitude, but opposite in sign. Therefore, they cancel when unpolarized light is used. For a symmetrical cone of light incident upon an untilted filter they cancel as well, because the roles

of S and P polarization are interchanged in any two perpendicular cross sections of the cone. Hence, Fresnel reflectance effects are observable only when polarized light is used, and when the filter is tilted.

Because of the opposing effects of S and P polarization in two mutually orthogonal planes, the effective value of θ'^2 to be used in this case, in the last term of eq (13a), is the difference of the two values in (14a, b). Therefore,

$$\tau - T = \pm \tau \gamma_r \theta_T^2$$

$$= \pm 4\tau (n'/n) r \theta_T^2, \qquad (16)$$

where the two signs pertain to the two cases in which the light is S or P polarized in the tilt plane.

This error is largest for large transmittances. If $n = 1.5$, $n' = 1$, $r = 0.04$, and $\tau = 0.92$, its magnitude is $\tau - T = 0.1\ \theta_T^2$, which is also plotted in figure 7. The figure shows that the Fresnel-reflectance error is of the same order of magnitude as the path-length error.

According to figure 10 the magnitude of this effect remains the same when a thin surface layer is present on the sample. The solid lines show the Fresnel reflectances for S and P polarization and for $n = 1.5$, $n' = 1$. As indicated by the broken lines, a thin layer of index $n_1 = 1.4$ and thickness $\lambda/100$ merely shifts these curves by a small amount. Thus, the angular dependence predicted by eq (16) remains unchanged, only the factor, r, on the right-hand side is changed insignificantly.

D. Elimination of Beam-Geometry Errors

The obliquity errors discussed in the previous section cannot be eliminated experimentally. In fact,
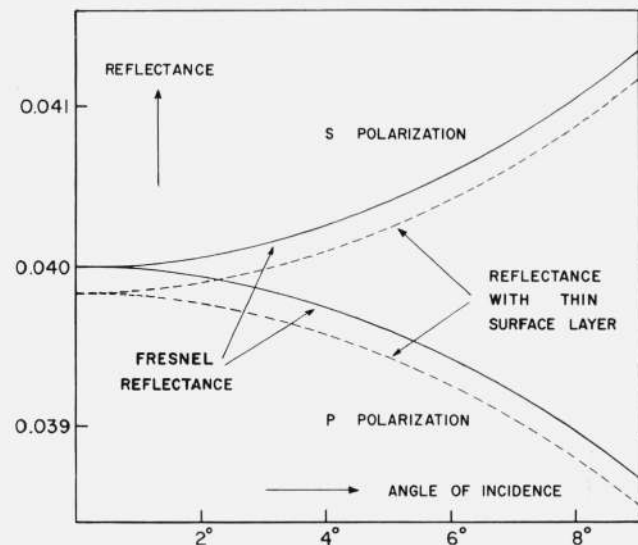

FIGURE 10. Computed reflectance of dielectric boundary ($n = 1.5$, $n' = 1$) with and without thin surface layer of thickness $\lambda/100$ and index 1.4.

they are increased by the necessity of tilting the sample in order to reduce the interreflection error. However, these obliquity errors can be predicted quantitatively and may, therefore, be removed by numerical correction of measured transmittances.

Thus, it should be possible to perform accurate measurements of 'true' transmittance with a conventional focused-beam spectrophotometer by eliminating defocusing and interreflection errors as indicated, measuring the tilt angle, and then applying a correction term, such as given by eqs (15) and (16) [13].

The same goal may be accomplished, in a much simpler fashion, by measuring in collimated rather than focused light. However, this cannot be done by simply repositioning the two lenses to make the light between them parallel. Such a beam geometry would still suffer from interreflection effects, so that the necessity to tilt the sample would reintroduce beam displacement and obliquity errors.

In order to avoid interreflections, it is necessary to use off-axis mirrors to collimate the light, and refocus it into the detector, as shown in figure 11. In this case, no significant portion of the light reflected from the sample will reach the detector, provided that the sample is normal to the beam and that off-axis mirrors are used in the monochromator as well. Each successive optical element will then reflect this light further toward the source, until some of it is returned by some lens on the source side of the monochromator. The final amount reaching the detector will be negligibly small.

To ensure that these conditions are realized, the imaging properties of the system must be quite good. Since a well-collimated beam cannot be derived from an extended source, it is necessary to equip the monochromator with small circular entrance and exit apertures rather than slits. Off-axis parabolas must be used rather than spherical mirrors to provide good imaging, so that the reflected light will still "fit" the monochromator apertures.

In addition, it is necessary to reduce the effects of spurious reflections by baffling, and by blackening of all component parts. The system must be aligned very carefully. This may be accomplished by means of an alignment laser and precision leveling devices for all components, including the sample holder.

The new spectrophotometer mentioned in section II, above, was designed and constructed in accordance with these guide lines. Returning the reflected light through the monochromator apertures was found to be a relatively easy alignment which, in addition to eliminating interreflections, also ensures that the samples are normal to the beam to within 1 milliradian. Therefore, no measurable obliquity errors are encountered and beam displacements will not occur, either. Unlike a focused-beam spectrophotometer, this instrument measures "true" transmittance without the necessity for elaborate precautions and numerical corrections.

The fact that this spectrophotometer is indeed effectively free from interreflection errors is demonstrated in figure 12. The figure shows the results of a
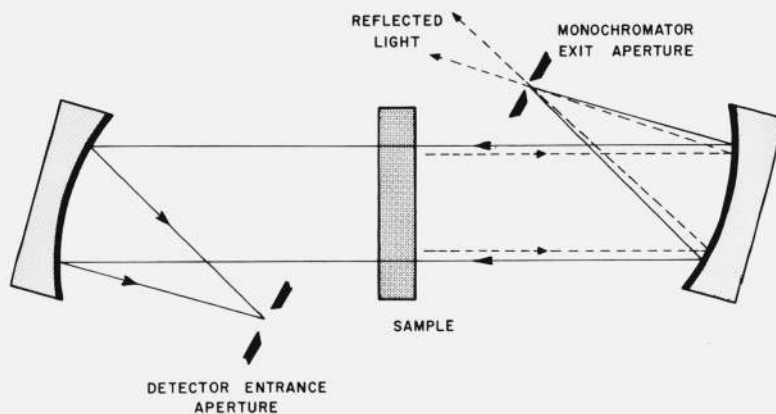
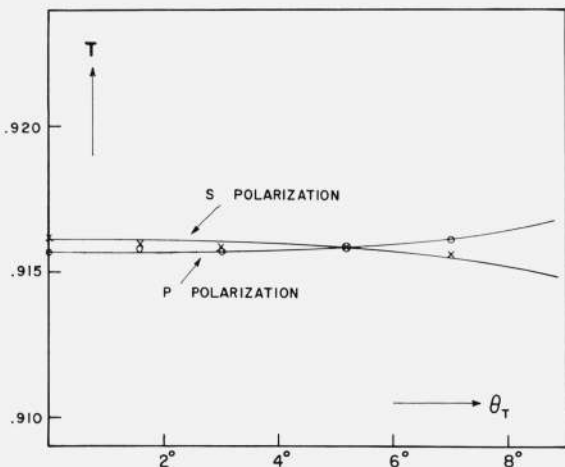FIGURE 11. Elimination of interreflections by using collimated light at normal incidence and off-axis mirrors.

FIGURE 12. Measured transmittance T versus tilt angle for clear quartz sample between off-axis mirrors.

FIGURE 13. Measured interference effect for thin sample at near-infrared wavelengths.

tilting experiment similar to that of figure 8. There is no 'interreflection hump' near normal incidence as in the previous case, and the average of the measured transmittances for S and P polarization is the same for all tilt angles. The particular sample used (a clear quartz plate) was found to be slightly birefringent. This was verified by checking it between crossed polaroids.

VI. Interference Effects

Figure 13 demonstrates the possibility of interference effects in spectrophotometry. A recording spectrophotometer was used to measure the transmittance of a very thin glass plate ($nt \sim 0.24$ mm) at near-infrared wavelengths ($\lambda \sim 1.05$ μm). The observed modulation of transmittance of roughly 1 percent, due to interference fringes spaced 2.3 nm apart, is significantly smaller than would be expected from eq (5a), which predicts a fringe visibility of about 8 percent for this particular case. As already mentioned, this discrepancy arises from the partial coherence of the illuminating light.
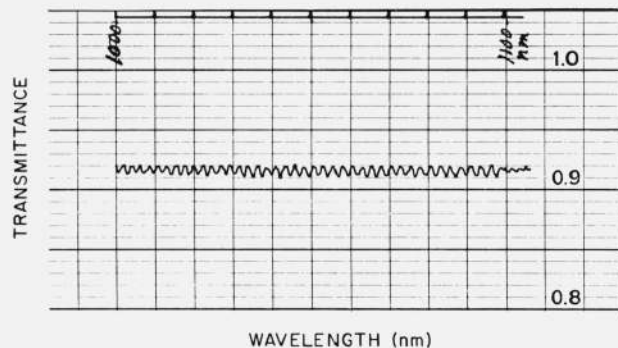
Due to various 'smearing factors', such as localization of fringes, unequal amplitudes of interfering beams, and imperfect temporal or spatial coherence of the spectrophotometer beam, the effect is likely to be small in most practical situations. The particular type of interference observed and its magnitude are sample-dependent, and are also a function of the beam geometry of the spectrophotometer.

Unless the sample is plane-parallel by interferometric standards, the interference pattern will be of the Fizeau type, and will be localized in the sample. These fringes will be 'seen' to a greater extent by the detector of a focused-beam spectrophotometer (fig. 14a) than by that of a parallel-beam instrument. On the other hand, the latter is more susceptible to the Haidinger rings localized at infinity (fig. 14b) which occur when the sample is plane-parallel and is normal to the beam. Both types of fringes may result in a modulation of measured transmittance, such as shown in figure 13, when the spectrophotometer wavelength is scanned. The Fizeau fringe pattern may also cause a similar modulation of transmittance when the sample is moved across the beam at a fixed wavelength setting.

For most samples the reflectance r at the sample boundaries is small. Thus, two-beam rather than multiple-beam interference will be observed, and the fringe contrast will be small because of the large ratio

464

1/r of the amplitudes of the two interfering beams. A further reduction of contrast may be attributed to the
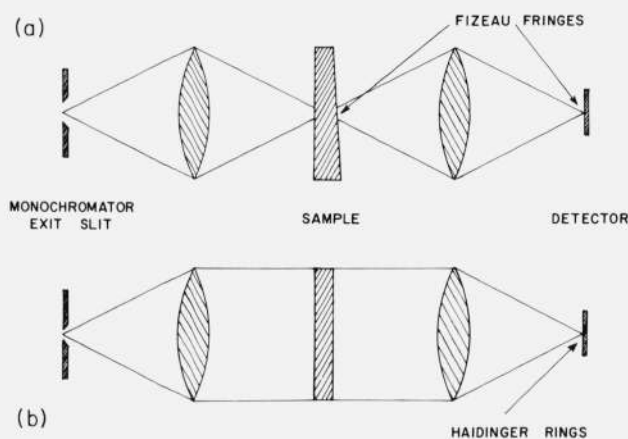

FIGURE 14. Localization of (a) Fizeau fringes, and (b), Haidinger rings in focused-beam and collimated-beam spectrophotometers.

finite degree of coherence of the interfering beams. The effect of imperfect temporal coherence is that the spectral fringe spacing, $\delta\lambda$, is generally significantly smaller than the bandpass $\Delta\lambda$ of the monochromator, so that the remaining net effect will be a much subdued average over several fringes. For example, $\delta\lambda = 0.04$ nm for a 2-mm filter of refractive index $n = 1.5$ at $\lambda = 500$ nm, whereas the normally used bandpass of the spectrophotometer described in section 2 is $\Delta\lambda = 0.8$ nm. In this case, the detector averages over twenty fringes and the reduction of contrast is at least twentyfold. Lack of perfect spatial coherence may similarly lead to an averaging of several spatially separated fringes comprised within the spot size seen by the detector.

The over-all effect of these various factors is difficult to assess. Within the context of this paper it is only possible to estimate an upper bound of the effect on transmittance measurements with the spectrophotometer described here. Assuming the case of a perfectly plane-parallel, clear sample of optical thickness nt, arranged perfectly normal to the beam, the measured transmittance is [14]

$$T = \tau \left[1 + 2r \mid \gamma_{12} \mid \cos\left(\frac{4\pi}{\lambda} nt + \alpha_{12} \right) \right] \quad (17)$$

where τ is the average transmittance, r is the Fresnel reflectance of the sample boundaries, and

$$\gamma_{12} = \mid \gamma_{12} \mid e^{i\alpha_{12}} \quad (18)$$

is the complex degree of coherence of the interfering beams. The theory of partial coherence permits the computation of $\mid \gamma_{12} \mid$ as a function of the beam parameters [15]. For this particular spectrophotometer such computations show, for example, that a variation of measured transmittance as large as 3×10^{-3} transmittance units is possible for a sample of optical thickness 3mm measured at 500 nm and 0.8 nm bandwidth.

This result, although a worst-case estimate, indicates that interference must be reckoned with in high-accuracy spectrophotometry. The presence or absence of an effect should be ascertained experimentally whenever indicated. If present, the interference effect should be measured, and then averaged to obtain the 'true' transmittance of the sample.

Generally, the effect is largest for thin samples, small bandwidths, and long wavelengths. Thus, only sufficiently thick filters should be used as transfer standards for the assessment of spectrophotometric accuracy. Neutral-density filters are preferable since they permit the use of large bandwidths.

VII. Nonlinearity Correction

All spectrophotometers are subject to nonlinearity errors which must be eliminated by applying a correction, ΔT, converting the measured transmittance, T, into the true value

$$\tau = T + \Delta T. \quad (19)$$

A simple and yet accurate method to determine this correction is the method of light addition, based upon the fact that a linear system which gives readings $I(A)$ and $I(B)$ for radiant fluxes A and B will give a reading $I(A+B) = I(A) + I(B)$ when the two fluxes are added incoherently. The system is nonlinear and a correction must be applied if the ratio

$$1 + \sigma(A, B) = \frac{I(A+B)}{I(A) + I(B)} \quad (20)$$

is not equal to unity. The most practical implementation is the double-aperture method due to Clarke [3], in which the two fluxes are those transmitted by a pair of apertures which may be opened and closed separately or in combination. This method was used in the present work, and is discussed in detail in references [16] and [17].

The nonlinear detector response may be expressed in the form

$$I(\phi) = \eta\phi[1 + \epsilon(\phi)], \quad (21)$$

where

$I(\phi) = $ signal current minus dark current,

465

η = nominal detector sensitivity,
ϕ = radiant flux,
$\epsilon(\phi)$ = departure from linearity.

If the two apertures are equal in size, and if $\phi = A + B$ is the combined flux through both apertures, then, eq (20) may be written as

$$1 + \sigma(\phi) = \frac{I(\phi)}{2I(\phi/2)} = \frac{1 + \epsilon(\phi)}{1 + \epsilon(\phi/2)}. \qquad (22)$$

The measured apparent transmittance for a sample with true transmittance, τ, is

$$T = \frac{I(\tau\phi)}{I(\phi)} = \tau \frac{1 + \epsilon(\tau\phi)}{1 + \epsilon(\phi)}, \qquad (23)$$

so that the required additive correction ΔT of eq (19) is given by

$$\Delta T = \tau \left[1 - \frac{1 + \epsilon(\tau\phi)}{1 + \epsilon(\phi)} \right]. \qquad (24)$$

These equations show that there is no straighforward functional relationship between the double-aperture datum, σ, and the nonlinearity correction ΔT. The former samples the detector response at the two points ϕ and $1/2\ \phi$, but for the latter, we require the knowledge of $\epsilon(\phi)$ at a different pair of points, ϕ and $\tau\phi$. In the usual application of the double-aperture method, this difficulty is circumvented by using the fact that the multiplier of τ on the right-hand side of (23) happens to be the reciprocal of the right-hand side of (22), if $\tau = 1/2$. Thus, $[1 + \sigma(\phi)]$ is the multiplicative correction to be applied when $\tau = 1/2$. Similarly, the correction factor for $\tau = 1/4$ is $[1 + \sigma(\phi)][1 + \sigma(1/2\ \phi)]$, and for $\tau = 1/2^n$ it is

$$\tau/T = \prod_{\nu=1}^{n} [1 + \sigma(\phi/2^{n-1})]. \qquad (25)$$

Thus, one can measure $\sigma(\phi)$, $\sigma(1/2\ \phi)$, . . . calculate the corresponding multiplicative corrections for $\tau = 1/2, 1/4, \ldots$, and then draw a curve from which the correction may be read for arbitrary values of τ. This method is unsatisfactory because:

(a) The actually measured corrections are unevenly distributed along the τ-axis, with wide gaps between them in the regions of most interest.

(b) Most measurements are made at low light levels, where the correction is small and the experimental error is large.

(c) Each measured point depends on the previous ones, so that the errors accumulate as τ is decreased.

(d) The necessity to read the correction from a graph is awkward, especially if all other data are processed by computer.

These disadvantages can be overcome since, according to (22) and (24), ΔT is linked to σ through $\epsilon(\phi)$.

Hence, it is possible to measure $\sigma(T\phi)$ for evenly distributed values of τ, process these data to find $\epsilon(\phi)$, and then calculate ΔT directly from (24). In order to do so, a lamp current is chosen so that the unattenuated flux, ϕ, through both apertures corresponds to the 100 percent point of the transmittance scale. After $\sigma(\phi)$ has been measured, the incident flux is attenuated in four 20 percent steps, and $\sigma(\tau\phi)$ is measured for $\tau = 0.8, 0.6, 0.4$, and 0.2. This series of measurements is repeated four times.

An example of the data so obtained is shown in figure 15. In all cases, the dependence of σ on T could
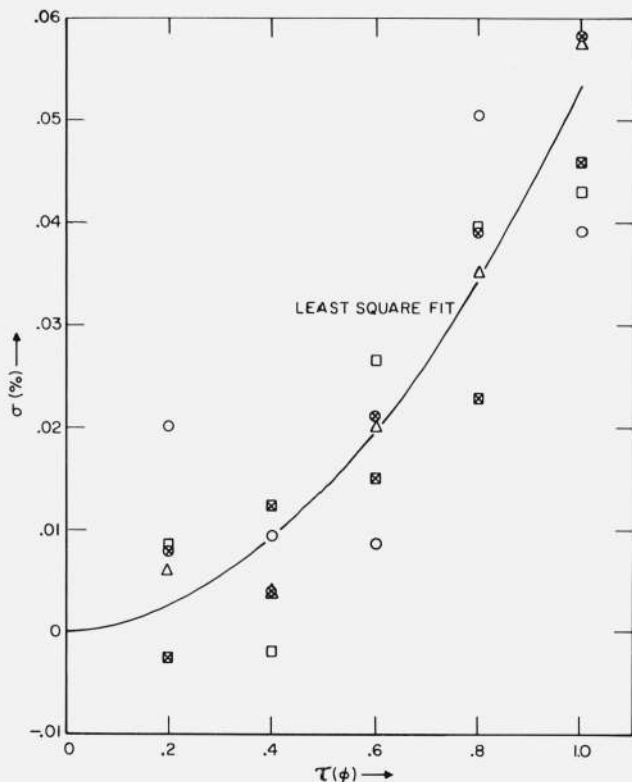

FIGURE 15. Measured dependence of the nonlinearity datum $\sigma(\tau\phi)$ on τ for $I(\phi) = 3 \times 10^{-7}A$ and $\lambda = 525$ nm.

be represented satisfactorily in the form of a parabola,

$$\sigma(\tau\phi) = a\tau + b\tau^2, \qquad (26)$$

$$a = a(\phi), \quad b = b(\phi), \qquad (27)$$

where the coefficients, a and b, are determined from the measured data by least-square fitting, using the inverse variances of the measured values of $\sigma(\tau\phi)$ as weight factors. The use of a second-degree equation was justified by a statistical analysis with the residuals showing no patterns suggesting higher order terms.

Hence, we can calculate ΔT as follows. Letting

$$\epsilon(\phi) = \alpha\tau\phi + \beta(\tau\phi)^2 + \ldots \qquad (28a)$$

466

and then using eq (22), we find

$$\sigma(\tau\phi) = 1/2\ \alpha\tau\phi + 1/4(3\beta - \alpha^2)\ (\tau\phi)^2 + \ . \ . \ . \qquad (28b)$$

to second order in ϕ, so that

$$a = 1/2\ \alpha\phi, \qquad b = 1/4(3\beta - \alpha^2)\phi^2, \qquad (28c)$$

according to (26, 27). Solving for α and β, and substituting the result into (28a),

$$\epsilon(\phi) = 2a\tau + 4/3(a^2 + b)\tau^2 + \ . \ . \ . \qquad (28d)$$

and, therefore,

$$\Delta T = \frac{2aT(1 - T) + 4/3(a^2 + b)T(1 - T)^2}{1 + 2a + 4/3(a^2 + b)}, \quad (29)$$

upon substitution of (28d) into (24) for $\tau = T$ and $\tau = 1$.

Thus the coefficients, a and b, can be stored in the computer after $\sigma(\tau\phi)$ was measured as described, and then ΔT may be calculated from eq (29) as required for arbitrary values of the measured apparent transmittance T.

As an indication of the precision of this method, table 3 lists the results obtained in two independent determinations of the nonlinearity correction. The two sets of final results for σ are in far better mutual agreement than the individual raw data of figure 15. The residual discrepancies of the additive correction, ΔT, never exceed 10^{-5} transmittance units.

For the particular spectrophotometer described in section II the nonlinearity correction was found to be independent of source polarization, free from interference effects, but slightly dependent on wavelength. This variation with wavelength (about 5×10^{-5} transmittance units or less between 400 and 750 nm) is taken into account in all measurements by means of a numerical interpolation formula derived from the measured values of ΔT for three wavelengths.

TABLE 3. Repeated measurements of σ and $\Delta T(\lambda = 525\,\mathrm{nm}, I(\phi) = 3 \times 10^{-7}\,\mathrm{A})$

T	First measurement		Second measurement	
	$\sigma \times 10^4$	$\Delta T \times 10^4$	$\sigma \times 10^4$	$\Delta T \times 10^4$
0.1	0.07	0.72	0.19	0.77
.2	.25	1.38	.45	1.46
.3	.52	1.96	.79	2.02
.4	.91	2.40	1.21	2.43
.5	1.39	2.67	1.70	2.66
.6	1.97	2.73	2.27	2.68
.7	2.66	2.53	2.92	2.45
.8	3.45	2.04	3.65	1.95
.9	4.34	1.21	4.45	1.14
1.0	5.34	0.00	5.33	0.00

VIII. References and Notes

[1] Mavrodineanu, R. J. Res. Nat. Bur. Stand. (U.S.), 76A (Phys. and Chem.), No. 5, 405 (Sept.–Oct. 1972).

[2] Hawes, R. C., Appl. Optics 10, 1246 (1971).

[3] Clarke, F. J. J., J. Res. Nat. Bur. Stand. (U.S.), 76A (Phys. and Chem.), No. 5, 375 (Sept.–Oct. 1972).

[4] Mielenz, K. D., Eckerle, K. L., Madden, R. P., Reader, J., Appl. Optics (to be published).

[5] Mielenz, K. D., and Eckerle, K. L., Nat. Bur. Stand. (U.S.), Tech Note 729, 60 pages (June 1972).

[6] Taylor, D. J., Rev. Sci. Instr. 40, 559 (1969).

[7] Born, M., and Wolf, E., Principles of Optics (Third Edition, Pergamon Press, 1965), Chapters 1 and 13.

[8] In all practical applications the surrounding medium is air. Most refractometers measure refractive indices with respect to air. In this case, the dependence of τ on n' is taken into account.

[9] Vasicek, A., Optics of Thin Films (North-Holland Publishing Co., 1960), Chapter 3.

[10] For $n' = 1$, $n = 1.5$, and $n_1 = 1.4$, the numerical value of this factor is -0.02. In addition, $\sin^2(x/2)$ is small for a very thin film. Further computations on this subject are presented in figure 10.

[11] Mavrodineanu, R., private communication.

[12] These measurements were performed by R. J. Bruening, NBS, on a goniophotometer with lenses for $\lambda = 546.1$ nm.

[13] It should be noted that the simplifying assumptions which led to eqs (13) and (14) may not apply. The correction terms must be derived for each spectrophotometer individually. A detailed knowledge of beam geometry is necessary for this purpose.

[14] Born, M., and Wolf, E., Principles of Optics (Third Edition, Pergamon Press, 1965), Chapter 10.

[15] Equation (19) was derived from the general expressions for $|\gamma_{12}|$ for small quasimonochromatic sources derived in K. D. Mielenz, Gas Lasers and Conventional Sources in Interferometry (Electron Beam and Laser Beam Technology, Academic Press, N.Y., 1968). For a uniformly illuminated circular aperture of angular radius $\alpha = a/2f$, the degree of spatial coherence is given by

$$|\gamma|_{\text{spatial}} = |(\sin A)/A|$$

where $A = k_0\alpha^2 t/2$, $k_0 = 2\pi/\lambda$. The degree of temporal coherence is the normalized Fourier transform of the spectral profile transmitted by the aperture, which in this case is

$$F(k = k_0) = \begin{cases} \sqrt{\dfrac{1}{4}a^2 - x^2} & \text{if } x^2 \leq \dfrac{1}{4}a^2, \\ 0 & \text{otherwise,} \end{cases}$$

where $x = (k - k_0)dx/dk$ is the linear coordinate in the aperture plane, and where the aperture diameter is assumed to be much larger than the Rayleigh width of the grating. This leads to

$$|\gamma|_{\text{temporal}} = |2J_1(B)/B|,$$

where $B = atdk/dx$. Expressing $|\gamma_{12}|$ as the product of the degrees of spatial and temporal coherence, and substituting the result into (17), we obtain the numerical results quoted in section VI.

[16] Sanders, C. L., J. Res. Nat. Bur. Stand. (U.S.) 76A (Phys. and Chem.), No. 5, 437 (Sept.–Oct. 1972).

[17] Mielenz, K. D., and Eckerle, K. L., Appl. Optics, 11, 2294 (1972).

(Paper 76A5–732)